

# Gravitational Wave Emission by Cataclysmic Variables: numerical models of semi-detached binaries.

Luciano Rezzolla<sup>1,2</sup>, Kōji Uryū<sup>1,3</sup>, & Shin’ichirou Yoshida<sup>1</sup>.

<sup>1</sup>SISSA, International School for Advanced Studies, Via Beirut 2-4, 34014 Trieste, Italy,

<sup>2</sup>INFN, Department of Physics, University of Trieste, Via Valerio 2, 34127 Trieste, Italy,

<sup>3</sup>Department of Physics, University of Wisconsin-Milwaukee, P.O. Box 413, Milwaukee, WI 53201, U.S.A.

Received / Accepted

## ABSTRACT

Gravitational wave emission is considered to be the driving force for the evolution of short-period cataclysmic binary stars, making them a potential test for the validity of General Relativity. In spite of continuous refinements of the physical description, a 10% mismatch exists between the theoretical minimum period ( $P_{\text{turn}} \simeq 70$  min) and the short-period cut-off ( $P_{\text{min}} \simeq 80$  min) observed in the period distribution for cataclysmic variable binaries. A possible explanation for this mismatch was associated with the use of the Roche model. We here present a systematic comparison between self-consistent, numerically constructed sequences of hydrostatic models of binary stars and Roche models of semi-detached binaries. On the basis of our approach, we also derive a value for the minimum period of cataclysmic variable binaries. The results obtained through the comparison indicate that the Roche model is indeed very good, with deviations from the numerical solution which are of a few percent at most. Our results therefore suggest that additional sources of angular momentum loss or alternative explanations need to be considered in order to justify the mismatch.

**Key words:** binaries: close – stars: low-mass – hydrodynamics – gravitation

## 1 INTRODUCTION

Semi-detached binary systems composed of a white dwarf as the primary and a low-mass main sequence star or brown dwarf as the secondary, are usually referred to as Cataclysmic Variables, or CVs (Warner 1995). Such systems could show a cataclysmic behaviour as a consequence of mass overflow from the secondary to the primary star. The observed orbital period distribution of these systems has two distinctive features: (a) a statistically significant deficit of systems with orbital periods between 2 and 3 hours, known as the “period gap”; (b) a sharp lower cutoff at an orbital period of  $P_{\text{min}} \simeq 80$  min which is referred to as the “minimum period” (Ritter & Kolb 1998).

In modeling short-period CVs (i.e. CVs with an orbital period  $< 2$  hr), it has long been proposed that gravitational radiation reaction drives their evolution enabling a continuous mass flow to occur from the secondary to the primary star (Kraft, Mathews & Greenstein 1962; Paczyński 1981; Paczyński & Sienkiewicz 1981; Rappaport, Joss & Webbink 1982; D’Antona & Mazzitelli 1982; Paczyński & Sienkiewicz 1983; Nelson, Chau & Rosenblum 1985; Kolb & Ritter 1992; Howell, Rappaport & Politano 1997; Kolb & Baraffe 1999). This feature makes CVs a potential test of General Relativity (Paczynski & Sienkiewicz 1983) <sup>\*</sup>.

The evolutionary scenario for a short-period CV can be summarized as follows. Consider a binary system with the secondary star having a mass  $0.1M_{\odot} \lesssim M_2 \lesssim 0.3M_{\odot}$  <sup>†</sup>. As a result of the binary evolution, the system becomes semi-detached, with the secondary star filling its “critical lobe” (which is defined here as the three-dimensional equipotential surface having a cusp at the inner Lagrangian point) <sup>‡</sup>. The loss of angular momentum then induces a mass overflow from the inner Lagrange point onto the primary degenerate dwarf. For the particular class of CVs known as Dwarf Novae an accretion disc is formed around the primary dwarf star and it is this which is responsible for the observed “cataclysmic” behaviour.

During the initial stages of the binary evolution, the mass-transfer timescale  $\tau_{\dot{M}}$ , which is of the same order as the timescale for angular momentum loss due to the gravitational wave emission  $\tau_{\text{GR}}$ , is much longer than the Kelvin-Helmholtz timescale  $\tau_{\text{KH}}$ . Under these conditions, the secondary can maintain its thermal equi-

<sup>†</sup> A slightly different evolution scenario should be considered in the case in which  $M_2 \lesssim 0.1M_{\odot}$  (Paczynski 1981).

<sup>‡</sup> We here introduce the term “critical lobe” in order to distinguish between the critical equipotential surface obtained from a self-consistent three-dimensional solution of the hydrodynamical equations and the corresponding surface obtained when using the Roche model and which is usually referred to as the “Roche-lobe”.

<sup>\*</sup> Note that for CVs with an orbital period  $> 3$  hr the emission of gravitational waves cannot drive the binary evolution.

librium and it slowly moves down the main sequence as it loses mass. As a result of angular momentum loss, the orbital period of the binary system decreases and the mean density of the secondary increases. A direct consequence of this is that  $\tau_{\text{KH}}$  for the secondary also increases.

Because in the course of the evolution the ratio  $\tau_{\dot{M}}/\tau_{\text{KH}}$  decreases secularly, the secondary gets more and more out of thermal equilibrium. This is connected with a tendency of the star to shrink less and less or even to expand upon mass loss, depending on the value of  $\tau_{\dot{M}}/\tau_{\text{KH}}$ . The minimum (turning) period of the binary orbit  $P_{\text{turn}}$  is reached for a specific value of the ratio  $\tau_{\dot{M}}/\tau_{\text{KH}}$  which depends somewhat on the model assumed for the secondary [cf. eq. (2)]. After the minimum period is reached, the nuclear burning becomes inefficient and radiative losses from the surface of the star will reduce its heat content. Eventually the star expands despite losing mass and its evolutionary path moves away from the main sequence towards the degenerate star branch.

Within this evolutionary scenario,  $P_{\text{turn}}$  is usually determined by means of the so called Roche model, which we will discuss in more detail in Section 3.1. The minimum period found by several authors in this way (Paczynski 1981; Kolb & Ritter 1992; Howell, Rappaport & Politano 1997), turns out to be about 10 % shorter than the observed period cut-off  $P_{\text{min}}$  (see Kolb & Baraffe 1999 for the latest theoretical results). This difference seems to survive all attempts at introducing refined treatments of the stellar physics and of the stellar evolution.

There have been many proposals for solving this discrepancy between  $P_{\text{turn}}$  and  $P_{\text{min}}$ . One of the suggestions is that the finite size effects of the secondary star, that are neglected in the traditional Roche model, may not be negligible and might be responsible for the mismatch (Nelson, Chau & Rosenblum 1985; Kolb & Baraffe 1999; Lasota 2000). Indeed, Nelson et al. (1985) have claimed that when tidal distortion effects are included in their models on the basis of the scheme suggested by Chan & Chau (1979),  $P_{\text{turn}}$  is increased by  $\sim 10\%$ . These findings, however, were not confirmed by subsequent investigations (Kolb & Baraffe 1999).

In this paper, we focus our attention on the validity of the Roche model for calculating  $P_{\text{turn}}$  in CVs. For this doing, we compare the dynamical properties of semi-detached binaries obtained by means of the Roche model with those obtained by numerically solving the equations of hydrostatic equilibrium for a binary system. In our numerical approach, we solve exact equations for the hydrostatic equilibrium, so that the tidally deformed structure of the secondary star and the orbital motion of the binary system are computed self-consistently. This is a feature missing in the Roche model. In order to emphasize the differences which emerge from the hydrodynamics of the equilibrium binary system, our calculations do not include details of the thermal structure or evolution of the secondary.

The paper is organized as follows: in Section 2 we describe the assumptions made in the construction of the models for the binary system. In Section 3, we discuss the set of equations that is used in the numerical construction of the equilibrium sequences of binary stars. Sections 4 and 5 summarize the numerical results and present our conclusions.

## 2 ASSUMPTIONS OF THE MODELS

A number of assumptions are necessary for the construction of a model for a CV binary system. In particular, following Paczynski (1981), we consider a semi-detached binary system with

a white dwarf as the primary star with mass  $M_1$ , and a hydrogen rich star on the lower main sequence as the secondary star with mass  $M_2$ .  $M_1$  and  $M_2$  are assumed to be typically  $M_1 \simeq 0.5 - 1.0M_{\odot}$  and  $M_2 < 0.4M_{\odot}$ . Since the secondary is taken to be fully convective in this mass range, its structure is well described by a polytropic relation between the pressure  $p$  and the mass density  $\rho$

$$p = K\rho^{1+\frac{1}{N}}, \quad (1)$$

with polytropic index  $N = 3/2$  and polytropic coefficient  $K$ , which is constant in space for an isentropic model<sup>§</sup>. For such a polytrope, the condition for the occurrence of the minimum period can then be expressed as (D’Antona, Mazzitelli & Ritter 1989; Ritter 1996; Kolb & Ritter 1992)

$$\frac{\tau_{\dot{M}}}{\tau_{\text{KH}}} \sim 0.3. \quad (2)$$

This condition, which contains some uncertainties related to the stellar model assumed, will be used in Section 4.2 to determine the range of minimum periods from the numerically calculated values of the mass transfer timescale  $\tau_{\dot{M}}$ .

The radius of the primary is small compared to that of the secondary and the primary is therefore treated as a point-like mass. This simplifies the calculation of both the gravitational potential of the primary and its contribution to the quadrupole moment of the system [cf. eq (21)]. The binary orbit is assumed to be circular and the spin period of the secondary is taken to be synchronous with the orbital period. These are rather good approximations since the relaxation timescales to these states are much shorter than the evolutionary timescale of the system (Zahn 1975; Zahn 1977; Lecar, Wheeler & McKee 1976).

Finally, we assume that the secondary is always just filling its critical lobe and that the continuous mass-transfer from the secondary to the primary is conservative, so that the total mass of the system  $M = M_1 + M_2$  is constant in time. This latter assumption is justified when we consider the evolution of the binary system to be driven solely by the emission of gravitational radiation.

## 3 CONSTRUCTION OF THE MODELS

In this section we briefly discuss the two distinct sets of equations for the construction of models for the CVs. In Section 3.1, we summarize the set of equations describing the “standard” Roche model and in Section 3.2, we discuss the set of the equations for a numerically constructed hydrostatic model of a semi-detached binary.

### 3.1 Roche model of a semi-detached binary

We construct Roche models of CVs based on the Roche model of semi-detached binaries as discussed by Paczynski in 1981. In this approximation, the secondary star is assumed to fill up its Roche lobe and its gravitational field is treated as that of a point-like mass. Within this approach, it is convenient to measure the size of the Roche lobe through a mean radius  $r_L$  defined so that the sphere of radius  $r_L$  has the same volume  $V_0$  as the Roche lobe

$$r_L \equiv \left(\frac{3V_0}{4\pi}\right)^{\frac{1}{3}}. \quad (3)$$

<sup>§</sup> Note that  $K$  changes with  $q$  along the sequence of constant total mass equilibrium models.

The ratio of  $r_L$  to the binary separation  $a$  depends only on the mass ratio  $q \equiv M_2/M_1$  and the empirical expressions proposed by Paczyński (1971) and Eggleton (1983) are expressed as

$$\frac{r_L}{a} = f(q) = \begin{cases} \frac{2}{3^{\frac{1}{3}}} \left( \frac{q}{1+q} \right)^{\frac{1}{3}} & \text{(Paczyński 1971)} \\ \frac{0.49q^{\frac{2}{3}}}{0.6q^{\frac{2}{3}} + \ln(1+q^{\frac{1}{3}})} & \text{(Eggleton 1983)} \end{cases} \quad (4)$$

The above expressions are valid for the range of mass ratios of interest here:  $q \simeq 0.1 - 1$ . Paczyński's expression is accurate to within 1% when compared with the result obtained by numerical integration of the Roche-lobe (Kopal 1959). In the same range, Eggleton's expression is even more accurate.

Combining the above formula with Kepler's law

$$a^3 = \left( \frac{P}{2\pi} \right)^2 G(M_1 + M_2), \quad (5)$$

we obtain an expression for the orbital period  $P$  as

$$P = \frac{2\pi}{G^{\frac{1}{2}}} \left[ \left( \frac{r_L^3}{M_2} \right) \frac{q}{(1+q)(f(q))^3} \right]^{\frac{1}{2}}. \quad (6)$$

Within the Roche model, the spin angular momentum of the primary star is neglected and the total angular momentum  $J$  of the system is therefore given by

$$J = J_{\text{orb}} + J_{\text{spin}}, \quad (7)$$

where the orbital angular momentum of the system  $J_{\text{orb}}$  and the spin angular momentum of the secondary  $J_{\text{spin}}$  are defined respectively as,

$$J_{\text{orb}} = \left( Ga \frac{M_1^2 M_2^2}{M_1 + M_2} \right)^{\frac{1}{2}} = G^{\frac{1}{2}} \left[ \frac{r_L}{f(q)} \right]^{\frac{1}{2}} \left[ \frac{M_2^3}{q(1+q)} \right]^{\frac{1}{2}}, \quad (8)$$

and

$$J_{\text{spin}} = (r_g r_L)^2 M_2 \Omega = (1+q) f^2(q) r_g^2 J_{\text{orb}}. \quad (9)$$

Here  $r_g r_L$  is the radius of gyration of the secondary and for a polytrope with  $N = 3/2$ ,  $r_g \simeq 0.45$  (D'Antona, Mazzitelli & Ritter 1989). The theory of stellar structure provides a simple mass–radius relation which holds for lower main sequence stars in the mass range of interest here (see, for example, Kippenhahn & Weigert 1990). This relation can be written as

$$\frac{R_2}{R_\odot} = \chi \left( \frac{M_2}{M_\odot} \right)^\xi, \quad (10)$$

where  $M_\odot$  and  $R_\odot$  are the solar mass and the solar radius, respectively, and  $R_2$  is the radius of the lower main sequence star. For a star with chemical abundances similar to those of the Sun, we can set  $\chi = 0.83$  and  $\xi = 0.84$  (Kippenhahn & Weigert 1990). Moreover, as long as the star remains on the lower main sequence (i.e. as long as  $\tau_{\text{KH}} < \tau_{\text{M}}$ ), we can assume that the mass–radius relation (10) holds even in the presence of mass loss, i.e. when

$$r_L = R_2. \quad (11)$$

Using equations (10) and (11), we can now rewrite the expression for the orbital period (6) as

$$P = 2.78 \times \left[ \chi^3 \left( \frac{M_2}{M_\odot} \right)^{3\xi-1} \frac{q}{(1+q)(f(q))^3} \right]^{\frac{1}{2}} \text{ hr}, \quad (12)$$

and derive the two timescales which are relevant for the evolution of a CV binary: namely the timescale for gravitational wave emission  $\tau_{\text{GW}}$  and that for mass-transfer  $\tau_{\text{M}}$ . As mentioned above, we assume that the binary evolution is driven only by the emission of gravitational waves (GW) and the timescale for this to occur can be estimated by means of the standard quadrupole formula for two point-like masses orbiting around each other (Landau & Lifshitz 1975)

$$\begin{aligned} \tau_{\text{GW}} &\equiv \left( \frac{d \ln J}{dt} \Big|_{\text{GW}} \right)^{-1} \\ &= -\frac{5}{32} \left( \frac{P}{2\pi} \right)^{\frac{8}{3}} \frac{c^5}{G^{\frac{5}{3}}} \frac{(M_1 + M_2)^{\frac{1}{3}}}{M_1 M_2} \\ &= -7.87 \times 10^7 \left( \frac{P}{1 \text{ hr}} \right)^{\frac{8}{3}} \left( \frac{M_2}{M_\odot} \right)^{-\frac{5}{3}} [q^2(1+q)]^{\frac{1}{3}} \text{ yr}, \end{aligned} \quad (13)$$

On the other hand, we can calculate the mass-transfer timescale as

$$\tau_{\text{M}} \equiv - \left( \frac{d \ln M_2}{dt} \right)^{-1} = - \left[ \frac{d \ln M_2}{d \ln J} \frac{d \ln J}{dt} \Big|_{\text{GW}} \right]^{-1}, \quad (14)$$

where the logarithmic differential of the total angular momentum (7) can be expressed as

$$\begin{aligned} d \ln J &= \frac{1}{2} d \ln r_L + \frac{3}{2} d \ln M_2 \\ &\quad - \frac{1}{2} \left[ \frac{d \ln f(q)}{dq} + \frac{2q+1}{q(1+q)} \right] dq \\ &= \frac{1}{2} d \ln M_2 \left[ 2 - 2q - q(1+q) \frac{d}{dq} \ln f(q) + \xi \right], \end{aligned} \quad (15)$$

where we have used equations (10) and (11) as well as the conservation of the total mass of the system

$$dq = q(q+1) d \ln M_2. \quad (16)$$

Combining equations (13) – (15), we can write explicitly the mass-transfer timescale for the secondary as

$$\begin{aligned} \tau_{\text{M}} &= -\frac{1}{2} \left( \frac{d \ln J}{dt} \Big|_{\text{GW}} \right)^{-1} \\ &\quad \times \left[ 2 - 2q - q(1+q) \frac{d}{dq} \ln f(q) + \xi \right]. \end{aligned} \quad (17)$$

Note that the CV system described by the Roche model is determined in terms of two variables: the mass ratio  $q$  and the mass of the secondary,  $M_2$ .

### 3.2 Numerical hydrostatic model of a semi-detached binary

A numerical method for computing semi-detached compressible binaries in hydrostatic equilibrium has recently been developed by Uryū & Eriguchi (1999) [see also Uryū & Eriguchi (1998) for the case of incompressible binaries.]. Within the assumptions discussed in Section 2, and in a corotating reference frame, the matter of the secondary star satisfies the following equation of hydrostatic equilibrium (the Bernoulli equation)

$$-\frac{1}{2} \varpi^2 \Omega^2 + K(N+1)\Theta + \phi = C, \quad (18)$$

where,  $\phi$  and  $\Omega$  are the gravitational potential, and the angular velocity of the orbital motion, respectively.  $\varpi$  is the distance of the fluid element from the rotation axis of the binary and  $C$  is a constant. The function  $\Theta$  is defined by  $\rho = \Theta^N$ . The gravitational potential  $\phi$ , is computed using the integral expression

$$\phi(\mathbf{r}) = -G \int_{V_2} \frac{\rho(\mathbf{r}')}{|\mathbf{r} - \mathbf{r}'|} dV - \frac{GM_1}{|\mathbf{r} - \mathbf{r}_1|}, \quad (19)$$

where the volume integration is carried out in the interior of the secondary ( $V_2$ ), and  $\mathbf{r}_1$  is the position vector of the primary. Equations (18) and the integral in the equation (19) are discretized in a spherical coordinate system  $(r, \theta, \varphi)$  whose origin is at the centre of the secondary. Because of the symmetry of the configuration, we only compute the solution in the region  $r \in [0, R_0]$ ,  $\theta \in [0, \pi/2]$ ,  $\varphi \in [0, \pi]$ , where  $R_0$  is the maximum radius of a tidally deformed stellar surface. A solution is obtained on a grid with the number of gridpoints for each coordinate being  $(N_r, N_\theta, N_\varphi) = (65, 33, 65)$ . The Green's function of the integral in the equation (19) is expanded in Legendre polynomials  $P_\ell(\cos \theta)$  up to  $\ell = 14$ . The number of grid points as well as the number of Legendre polynomials used for the Green's function are chosen so as to provide satisfactory numerical accuracy and results presented in this paper have a numerical error which is typically less than 0.1%. [Further details of the numerical method can be found in Uryū & Eriguchi (1999) and references therein.]

In calculating models of “critical lobe-filling binaries” (hereafter critical lobe binaries), we first fix a value for the mass ratio  $q$  and then compute a set of solutions corresponding to different values of the orbital separation  $a$  (we start from a large initial value of  $a$  and then decrease it in steps of  $\delta a = R_0/50$ ). The sequence of solutions obtained in this way is terminated at an orbital separation for which the surface of the secondary star has a cusp at the inner Lagrange point. The corresponding configuration is identified as a critical lobe model for the given value of  $q$ . This procedure has been repeated for 31 models, changing  $q$  logarithmically in the range  $q \in [0.033, 1]$ .

For each of the 31 models, we compute the relevant timescales and, as in equation (13),  $\tau_{\text{GW}}$  is given by the rate of angular momentum loss from the system in the form of gravitational radiation (Misner, Thorne & Wheeler 1975),

$$\left. \frac{d \ln J}{dt} \right|_{\text{GW}} = -\frac{32G}{5c^5} \frac{\Omega^5}{J} (I_{11} - I_{22})^2. \quad (20)$$

The quadrupole moment tensor  $I_{ij}$  of the system is computed numerically as

$$I_{ij} \equiv \int_V (\rho_S + \rho_P) \left( x_i x_j - \delta_{ij} \frac{|\mathbf{r}|^2}{3} \right) dV, \quad (21)$$

where the volume  $V$  comprises both stars and  $\rho_S$ ,  $\rho_P$  are the mass densities of the secondary and primary stars, respectively, with the latter being expressed in terms of a three-dimensional Dirac delta function  $\rho_P \equiv M_1 \delta^3(\mathbf{r} - \varpi_1 \mathbf{e}_{x_1})$ . The vector  $\mathbf{r} = (x_1, x_2, x_3)$  is the position vector of a mass element and  $\varpi_1$  represents the distance of the primary star (a point particle) from the rotation centre of the binary. The vector  $\mathbf{e}_{x_1}$  is the unit vector along the  $x_1$  axis. The Latin indices in (21) run from 1 to 3 and correspond to the components of the Cartesian coordinate system whose origin is at the rotation centre of the binary system (the  $x_1$ -coordinate is oriented along the separation vector of the binary and the  $x_2$ -coordinate is in the orbital plane). The total angular momentum  $J$  for the model is computed as follows :

$$J = \int_{V_2} \rho \varpi^2 \Omega dV + M_1 \varpi_1^2 \Omega. \quad (22)$$

As in equation (14), we calculate the mass-transfer timescale as

$$\tau_M \equiv - \left( \frac{d \ln M_2}{dt} \right)^{-1} = \left( \frac{d \ln M_2}{d \ln J} \frac{d \ln J}{dt} \right)_{\text{GW}}^{-1}, \quad (23)$$

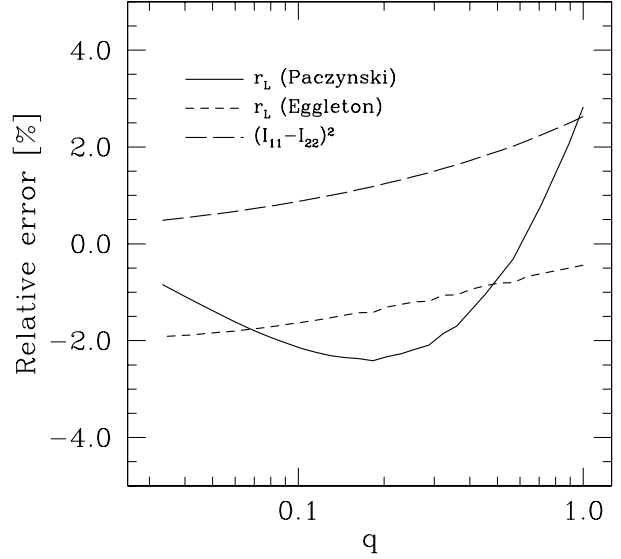


**Figure 1.** The relative differences of several quantities when computed using the Roche model and the numerical binary models are plotted against  $q$ . The solid line is the result for  $r_L$  as computed with Paczyński’s formula. The short-dashed line is the same but for Eggleton’s formula. The long-dashed line, is the relative error for  $(I_{11} - I_{22})^2$  [see eq. (21)].

where now the quantity  $d \ln M_2 / d \ln J$  is computed along the semi-detached equilibrium sequence from the expression

$$\frac{d \ln M_2}{d \ln J} = \frac{1}{q(q+1)} \frac{dq}{d \ln J}. \quad (24)$$

## 4 COMPARISON OF THE MODELS

In this Section, we compare the two classes of semi-detached binary models, namely the Roche model and the numerical critical lobe model in hydrostatic equilibrium. We first compare purely dynamical quantities for the two models. We then discuss the differences arising from the application of these two models to a cataclysmic binary system, focusing in particular on the differences in the mass-transfer timescale.

### 4.1 Comparison of dynamical properties

Two binaries are considered to represent the same physical system (and are therefore considered “comparable”) if they have the same mass ratio  $q$  and the same orbital period  $P$ . In practice, we first construct a numerical model of a critical lobe binary and then calculate the physical quantities of Roche model binary with the same mass ratio and orbital period. Note that the relation (10) between the mean radius and the mass of the secondary is not used in this comparison, but we match two different binaries on the basis of the dynamical timescale of the system (i.e. the orbital period of the binary system).

In the comparison we focus on: (a) the mean radius of the secondary  $r_L$ ; (b) the total angular momentum of the system  $J$ ; (c) the components of the quadrupole moment tensor  $(I_{11} - I_{22})^2$  and (d) the inverse of the timescale for gravitational wave emission

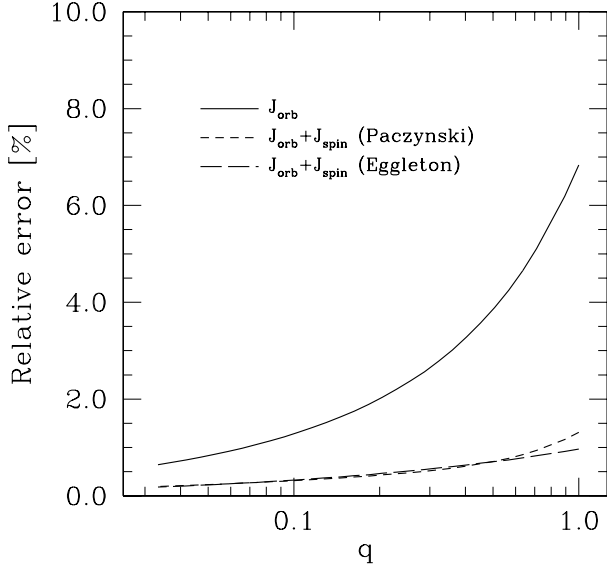


**Figure 2.** The relative deviations of the total angular momentum when computed using the Roche model and the numerical binary models are plotted against  $q$ . The solid line refers to binaries in which the spin angular momentum of the secondary is neglected in the Roche model. Binaries in which the spin contribution of secondary in the Roche model is instead included are indicated with a short-dashed line (for the case of Paczyński’s formula) and with a long-dashed line (for the case of Eggleton’s formula).

$d \ln J/dt$ . For all of these quantities we define the measure of the relative deviation as

$$\text{Relative error in } Q \equiv \frac{Q(\text{critical lobe}) - Q(\text{Roche model})}{Q(\text{Roche model})}, \quad (25)$$

and have plotted them in Figures 1-2 against the mass ratio of the system, and in Figure 3 against the orbital period.

In particular, the solid line in Figure 1 shows the mean radius of the critical lobe,  $r_L$ , from Paczyński’s formula, while the short-dashed line comes from using Eggleton’s formula. The long-dashed line, on the other hand, shows the relative error for  $(I_{11} - I_{22})^2$ . Similarly, Figure 2 shows the relative deviations of the total angular momentum: the solid line refers to binaries in which the spin angular momentum of secondary is neglected in the Roche model, while binaries for which the spin contribution of secondary in Roche model is included are indicated with short and long-dashed lines. Both Figures 1 and 2 show that for all of these quantities the errors made through the use of the Roche model are smaller than 3%, if the spin angular momentum of the secondary is taken into account.

In a similar way, in Figure 3, where we calculate the relative error in  $d \ln J/dt$  for different values of the orbital period, the different line types refer to two systems having a total mass of  $M = 0.8M_\odot$  and  $M = 1.3M_\odot$ , respectively. In this comparison we have used Eggleton’s formula but we have verified that the error is almost the same when Paczyński’s formula is used. Also in this case, the deviations are of at most a few percent, as found by Kolb & Baraffe (1999) when implementing the prescription of Chan & Chau (1979) for the corrections due to tidal distortion.

¶ We recall that in the Roche model  $I_{11} - I_{22} = a^2 M_1 M_2 / (M_1 + M_2)$ .

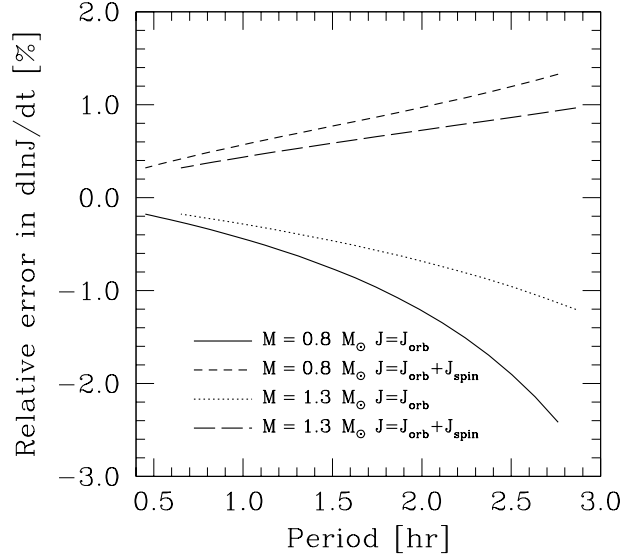


**Figure 3.** Relative error of the inverse of the timescale for angular momentum loss by gravitational radiation,  $d \ln J/dt$ . The solid line refers to a binary system with total mass  $M = 0.8M_\odot$  and does not include the spin angular momentum contribution of the secondary, which is instead included in the curve indicated with a short-dashed line. Similarly, the long-dashed and dotted lines are for a system having a total mass  $M = 1.3M_\odot$ , with and without the inclusion of the spin angular momentum of the secondary.

Note that in evaluating the timescale for the angular momentum loss, the accuracy of the Roche model increases as the mass of the secondary is decreased and thus for shorter orbital periods. This can be deduced from the fact that, for a fixed value of the total mass  $M$ , the relative error in  $d \ln J/dt$  becomes smaller for smaller orbital periods and therefore for smaller masses of the secondary. The improved accuracy is related to the fact that the Roche model is increasingly accurate as the finite-size effects become less and less important, or equivalently as the ratio  $r_L/a$  becomes smaller and smaller. In the case of Paczyński’s formula, this ratio can be expressed as

$$\frac{r_L}{a} = \frac{2}{3^{4/3}} \left( \frac{M_2}{M} \right)^{1/3}. \quad (26)$$

showing that for a fixed total mass  $M$ , finite-size effects will be smaller with a less massive secondary star.

## 4.2 Mass-transfer timescale

Next, we compare the mass-transfer timescale  $\tau_M$  computed from equations (13) and (17) for the Roche model binaries, and equations (20)–(24) for the numerical critical-lobe binaries. For the Roche model, we use Eggleton’s formula in equation (4). Note that the mass-radius relation (10) is used to compute  $\tau_M$ . In Figure 4, curves (i) and (ii) refer to a binary system with a total mass of  $0.8M_\odot$ , with the first one being the result of the fully numerical calculation and

the second one being obtained using the Roche model<sup>||</sup>. Curves (iii) and (iv) are similar to (i) and (ii), but refer to a system with total mass  $1.3M_{\odot}$ .

An important aspect emerging from Figure 4 is that, for all of the relevant masses of the secondary, the mass-transfer timescale computed numerically is slightly *larger* than that obtained from the Roche model. In other words, the Roche model slightly *underestimates* the evolutionary timescale, thus resulting in a *larger* minimum orbital period. As a consequence, our results indicate that a treatment which refines the hydrodynamic aspects of the critical lobe model for CVs produces even larger discrepancies with the observations.

In Figure 4, we also show the curves for a parametrized timescale  $\tilde{\tau}_{\text{KH}}$

$$\tilde{\tau}_{\text{KH}} \equiv \alpha \tau_{\text{KH}} = \alpha \frac{GM_2^2}{R_2 L_2}, \quad (27)$$

where the adjustable coefficient  $\alpha \in [0.25, 1.0]$  has been introduced to account for the uncertainty in the determination of the minimum period [cf. eq. (2)]

For a low-mass main sequence star, the luminosity of the secondary  $L_2$  appearing in (27) can be expressed as (Kippenhahn & Weigert 1990),

$$\frac{L_2}{L_{\odot}} = 0.1413 \left( \frac{M_2}{M_{\odot}} \right)^{2.25}. \quad (28)$$

The orbital period at which  $\tau_{\dot{M}} = \tilde{\tau}_{\text{KH}}$  corresponds to the minimum period of the binary system  $P_{\text{turn}}$ . In Tables I and II, we show the values of the binary parameters and the explicit values of  $P_{\text{turn}}$  at  $\tau_{\dot{M}} = \tilde{\tau}_{\text{KH}}$  for several values of  $\alpha$  and  $M$ .

## 5 CONCLUSIONS

The Roche model has been widely used in the literature to describe the dynamical evolution of CVs. The minimum periods computed on the basis of this model have shown a disagreement with observations and several attempts made to include more realistic descriptions of the system have not yet produced a satisfactory explanation for it. In order to assess the accuracy of the Roche model we have carried out numerical calculations of equilibria of corotating semi-detached binaries. The models obtained numerically are “exact” in the sense that they are hydrodynamically self-consistent and fully account for the finite size of the secondary star which fills its critical lobe.

However, when physical systems obtained with the two approaches are compared, these show only minimal differences which are always smaller than a few percent. Therefore, our results indicate that the explanation for the mismatch between the theoretical minimum period and the observed one must be due to something else. A better agreement with observations might be found when mechanisms that increase the efficiency of angular momentum loss from the system, are fully taken into account. Among these mechanisms one could consider, for instance, stellar winds or magnetic torques, both of which have been shown to be very efficient in removing angular momentum. An interesting alternative mechanism which could increase the angular momentum loss via gravitational

<sup>||</sup> For simplicity, we do not include here the spin angular momentum contribution of the secondary in the Roche model. As shown in Figure 3, this produces an additional error of a few percent at most.

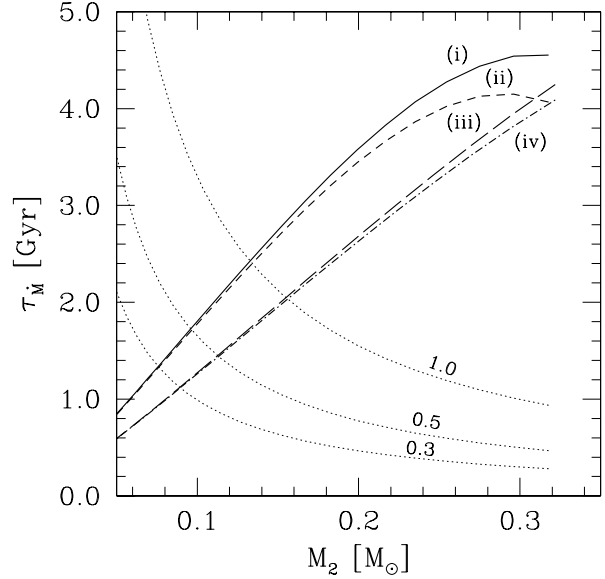


**Figure 4.**  $\tau_{\dot{M}}$  is plotted as a function of the mass of the secondary. Curves (i) and (ii) are for a binary system with a total mass of  $0.8M_{\odot}$ . Curve (i) corresponds to the result of the numerical computation, whereas (ii) is obtained with the Roche model based on the Eggleton formula. Curves (iii) and (iv) are similar to (i) and (ii), but for a system with total mass  $1.3M_{\odot}$ . Also plotted are the curves of  $\tilde{\tau}_{\text{KH}}$  for the secondary. The labels of these curves refer to the values of the parameter  $\alpha$  defined in equation (27).

model	$M_2/M_{\odot}$	$q$	$\tau_{\dot{M}}$ [Gyr]	$P_{\text{turn}}$ [min]
$\alpha = 0.25$				
Roche	0.0824	15.05	1.019	60.20
Numerical	0.0821	15.11	1.025	60.02
$\alpha = 0.3$				
Roche	0.0896	13.77	1.1174	64.28
Numerical	0.0893	13.83	1.119	64.08
$\alpha = 0.35$				
Roche	0.0962	12.77	1.208	67.96
Numerical	0.0958	12.83	1.204	67.74
$\alpha = 0.5$				
Roche	0.1133	10.68	1.442	77.22
Numerical	0.1127	10.74	1.449	76.92
$\alpha = 1.0$				
Roche	0.1561	7.483	2.034	99.12
Numerical	0.1550	7.540	2.049	98.58

**Table 1.** Comparison of binary parameters at the point along the evolutionary sequence where the relation,  $\tau_{\dot{M}} = \tilde{\tau}_{\text{KH}}$ , hold. The total mass of the system is  $1.3M_{\odot}$ .

model	$M_2/M_\odot$	$q$	$\tau_M$ [Gyr]	$P_{\text{turn}}$ [min]
$\alpha = 0.25$				
Roche	0.0702	10.67	1.215	53.66
Numerical	0.0698	10.72	1.201	53.45
$\alpha = 0.3$				
Roche	0.0763	9.725	1.330	57.28
Numerical	0.0759	9.785	1.311	57.05
$\alpha = 0.35$				
Roche	0.0820	8.997	1.437	60.58
Numerical	0.0815	9.055	1.412	60.31
$\alpha = 0.5$				
Roche	0.0967	7.471	1.714	68.88
Numerical	0.0960	7.528	1.727	68.52
$\alpha = 1.0$				
Roche	0.1341	5.109	2.401	88.56
Numerical	0.1328	5.172	2.427	87.90

**Table 2.** The same as Table 1, except that the total mass of the system is  $0.8M_\odot$

waves is given by the possible excitation of stellar oscillations in binary systems. These periodic perturbations, which could be excited in binary systems such as CVs, would generate gravitational wave emission which would add to the one coming from the orbital motion and, when resonant, could even be the largest source of gravitational radiation (Berti & Ferrari 2000).

## ACKNOWLEDGMENTS

We are grateful to Jean-Pierre Lasota for suggesting this research and for his useful comments, and to John Miller for carefully reading the manuscript. We also thank the referee, Hans Ritter, for his detailed suggestions. Financial support for this research has been provided by the MURST and by the EU Programme "Improving the Human Research Potential and the Socio-Economic Knowledge Base" (Research Training Network Contract HPRN-CT-2000-00137).

## REFERENCES

- Berti E., Ferrari V., Phys. Rev. D63 (2001) 064031  
 Chan K.L., Chau W.Y. 1979, ApJ, 233, 950  
 D'Antona F., Mazzitelli I., 1982, ApJ, 260, 722  
 D'Antona F., Mazzitelli, I., Ritter, H., 1989, A&A 225, 391  
 Eggleton P. P., 1983, ApJ, 268, 368  
 Howell S. B., Rappaport S., Politano M., 1997, MNRAS, 287, 929  
 Kippenhahn R., Weigert A., 1990, *Stellar Structure and Evolution*, Springer-Verlag, Berlin  
 Kopal Z., 1959, *Close Binary Systems*, Chapman and Hall, London  
 Kolb U., Baraffe I., 1999, MNRAS, 309, 1034  
 Kolb U., Ritter H., 1992, A&A, 254, 213  
 Kraft R. P., Mathews J., Greenstein J. L., 1962, ApJ, 136, L312  
 Landau L. D., Lifshitz E. M., 1975, *The Classical Theory of Fields*, 4th rev. ed., Pergamon, New York

- Lasota J-P., 2000, Talk given at the International Conference "Gravitational Waves: A Challenge to Theoretical Astrophysics.", Trieste  
 Lecar M., Wheeler J. C., McKee C. F., 1976, ApJ, 205, 556  
 Misner C. W., Thorne K. S., Wheeler J. A., 1970, *Gravitation*, Freeman & Co., San Francisco  
 Nelson L. A., Chau W. Y., Rosenblum A., 1985, ApJ, 299, 658  
 Paczyński B., 1971, ARA&A, 9, 183  
 Paczyński B., 1981, Acta Astron., 31, 1  
 Paczyński B., Sienkiewicz R., 1981, ApJ, 248, L27  
 Paczyński B., Sienkiewicz R., 1983, ApJ, 268, 825  
 Rappaport S., Joss P. C., Webbink R. F., 1982, ApJ, 254, 616  
 Ritter H., 1996, in: *Evolutionary Processes in Binary Stars*, eds. R.A.M.J. Wijers, M.B. Davies and C.A. Tout, NATO ASI Series C, Vol. 477, Kluwer Academic Publishers, p. 223  
 Ritter H., Kolb U., 1998, A&AS, 129, 83  
 Uryū K., Eriguchi Y., 1998, MNRAS, 299, 575  
 Uryū K., Eriguchi Y., 1999, MNRAS, 303, 329  
 Warner B., 1995, *Cataclysmic Variable Stars*, Cambridge University Press, Cambridge  
 Zahn J. -P., 1975, A&A, 41, 329  
 Zahn J. -P., 1977, A&A, 57, 383 ; erratum in 67, 162 (1978)